J Membrane Biol (2012) 245:283–290
DOI 10.1007/s00232-012-9449-z

# Electrical Transmission between Mammalian Neurons is Supported by a Small Fraction of Gap Junction Channels

**Sebastian Curti · Gregory Hoge · James I. Nagy · Alberto E. Pereda**

Received: 29 March 2012 / Accepted: 1 June 2012 / Published online: 24 June 2012


**Abstract** Electrical synapses formed by gap junctions between neurons create networks of electrically coupled neurons in the mammalian brain, where these networks have been found to play important functional roles. In most cases, interneuronal gap junctions occur at remote dendro–dendritic contacts, making difficult accurate characterization of their physiological properties and correlation of these properties with their anatomical and morphological features of the gap junctions. In the mesencephalic trigeminal (MesV) nucleus where neurons are readily accessible for paired electrophysiological recordings in brain stem slices, our recent data indicate that electrical transmission between MesV neurons is mediated by connexin36 (Cx36)-containing gap junctions located at somato–somatic contacts. We here review evidence indicating that electrical transmission between these neurons is supported by a very small fraction of the gap junction channels present at cell–cell contacts. Acquisition of this evidence was enabled by the unprecedented experimental access of electrical synapses between MesV neurons, which allowed estimation of the average number of open channels mediating electrical coupling in relation to the average number of gap junction channels present at these contacts. Our results indicate that only a small proportion of channels ($\sim$0.1 %) appear to be conductive. On the basis of similarities with other preparations, we postulate that this phenomenon might constitute a general property of vertebrate electrical synapses, reflecting essential aspects of gap junction function and maintenance.

**Keywords** Connexin36 · Electrical coupling · Electrical transmission · Gap junction

S. Curti (✉)
Facultad de Medicina, Departamento de Fisiología, Laboratorio de Neurofisiología Celular, Universidad de la República, Gral. Flores 2125, Montevideo 11800, Uruguay
e-mail: scurti@fmed.edu.uy

G. Hoge · A. E. Pereda (✉)
Dominick P. Purpura Department of Neuroscience, Albert Einstein College of Medicine, Bronx, NY 10461, USA
e-mail: alberto.pereda@einstein.yu.edu

J. I. Nagy
Department of Physiology, University of Manitoba, Winnipeg, Manitoba R3EOJ9, Canada

Gap junctions mediate electrical transmission between neurons by providing a pathway of low resistance for the spread of electrical currents and small metabolites (Bennett 1997). Contrasting initial perceptions and overcoming technical challenges and long-standing prejudices (Bennett and Pereda 2006), electrical synapses are now known to be present in virtually every structure of the mammalian brain, where they usually form networks of electrically coupled neurons (Bennett and Zukin 2004; Connors and Long 2004; Hormuzdi et al. 2004). However, and in marked contrast with some advantageous teleost model synapses (Pereda et al. 2004), the dendro–dendritic location of neuronal gap junctions in most brain structures (Connors and Long 2004) makes it difficult to correlate their physiological properties with anatomical features.

The mesencephalic trigeminal (MesV) nucleus, formed by the somata of primary afferents originating in jaw-closing muscles, constitutes one of the first examples supporting the presence of electrical synapses in the mammalian central nervous system (Hinrichsen and Larramendi 1970; Hinrichsen 1970; Baker and Llinás 1971; Llinas 1975). The demonstration of electrical coupling relied on indirect electrophysiological evidence obtained

by stimulating the peripheral projections of these afferents at a strength that was subthreshold for the recorded neuron, but was suprathreshold to others, thus allowing the detection of a depolarizing coupling potential, which represented the electrotonic spread of action potentials from electrically coupled cells (Hinrichsen 1970; Baker and Llinás 1971). Because of its limitations, this approach precluded a detailed analysis of the properties of these electrical synapses and the organization of electrical coupling within this nucleus. By combining tracer coupling analysis and immunochemistry with current electrophysiological approaches in rodent slices, we recently examined the properties, organization and developmental profile of electrical coupling between MesV neurons (Curti et al. 2012). Interestingly, we demonstrated that coupling between MesV neurons was mostly restricted to pairs (or very small clusters) of neurons and, in contrast with most examples where coupling decreases or disappears with age (Peinado et al. 1993; Meier and Dermietzel 2006), coupling was absent during early development and appeared at about postnatal day 8 to remain as a feature of the mature cellular phenotype of these neurons (Curti et al. 2012). In addition, we demonstrated that electrical transmission between MesV neurons is mediated by anatomically distinct somato–somatic contacts that contained, as with most mammalian electrical synapses (Bennett and Zukin 2004; Connors and Long 2004), the gap junction protein Cx36 (Curti et al. 2012).

Estimates obtained at mixed synapses formed by afferent terminals on the goldfish Mauthner cell (for review, see Pereda et al. 2004), where the number of channels was obtained from direct ultrastructural reconstruction of these terminals (Tuttle et al. 1986), suggested that only a small percentage of channels ($\sim$1 %) support the electrical component of a unitary mixed synaptic potential (Lin and Faber 1988). We review here evidence suggesting that, consistent with this finding, electrical transmission between mammalian neurons is also supported by a very small fraction of gap junction channels. Taking advantage of the uncommon experimental accessibility of MesV, we combined imaging-based estimates of numbers of channels present with physiological measurements and found that electrical coupling is supported by a surprisingly small fraction of conductive channels.

## Methods

For these experiments, Sprague Dawley or Wistar rats were used. Slicing and recording techniques were similar to those described previously (Curti et al. 2012). Detailed illustration and interpretation of electrophysiological recordings described here can be found in our previous report (Curti et al. 2012). Methods for tissue preparation and immunolabeling, sources of antibodies, and their specificity and analysis by confocal microscopy were as we previously described in studies of connexins in the central nervous system (Li et al. 2004a, b; Penes et al. 2005). Interpretations of images presented are also extensively described in our previous report (Curti et al. 2012). Statistical analysis is expressed as standard deviation (SD) or standard error of the mean (SEM).

## Results

Using in vivo single intracellular recordings, Baker and Llinás (1971) revealed the existence of electrical coupling between neurons of the MesV. We have more recently investigated the presence of electrical coupling between adjacent pairs of these neurons using paired-recordings in slices of rat brain stem visualized by IR-DIC (Fig. 1a). MesV neurons were identified by their large spherical somata and characteristic electrophysiological properties in response to current steps of both polarities (Pedroarena et al. 1999). The presence of electrical coupling was tested by recording membrane responses in two adjacent MesV neurons after the injection of hyperpolarizing current pulses in one of the cells. An example of a coupled pair is illustrated in Fig. 1b, in which a current pulse in the presynaptic cell evokes a membrane response in the postsynaptic cell of the same sign but of lower amplitude and slower temporal course. About 23 % of the explored pairs ($n = 243$) were electrically coupled. For each coupled pair, the coupling coefficient and junctional resistance were estimated and expressed as the average of the values in both directions (see Curti et al. 2012 for details) averaging $0.19 \pm 0.14$ SD and $6.2 \pm 6.33$ nS SD, respectively ($n = 47$). Estimates of junctional conductance in both directions for each pair showed a positive correlation with a slope of 1.04 ($R^2 = 0.75$) not significantly different than one ($p = 0.7$), indicating that gap junctional conductance between MesV neurons is largely nonrectifying (Curti et al. 2012).

### Somato–Somatic Contact Areas Contain Cx36

We next investigated by immunohistochemical approaches whether Cx36, a widespread neuronal connexin responsible for most electrical coupling in mammalian brain (Nagy et al. 2004; Meier and Dermietzel 2006; Condorelli 1998; Söhl et al. 1998), was expressed by MesV neurons of rats at postnatal day 15, corresponding roughly to the age at which electrophysiological studies of coupling between MesV neurons were conducted. At anterior levels through the MesV nucleus, neuronal somata are somewhat dispersed

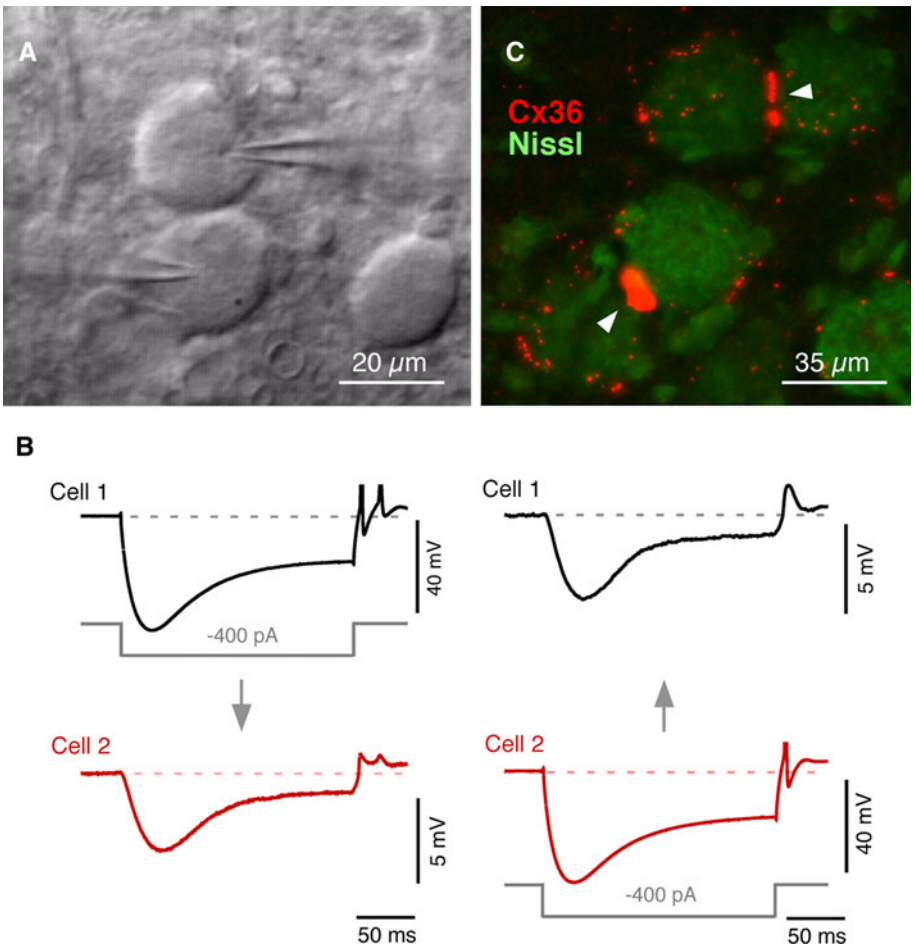


**Fig. 1** Electrical transmission between MesV neurons. **a** IR-DIC image of a pair of contiguous MesV neurons during a simultaneous whole-cell recording. **b** Simultaneous recording from a pair of electrically coupled MesV neurons. Voltage responses to 200 ms hyperpolarizing (400 pA) current pulses injected either in cell 1 (*left*) or cell 2 (*right*). **c** Immunofluorescence labeling of Cx36 associated with MesV neurons at postnatal day 15. Labeling for Cx36 is shown with *red fluorochrome* in sections counterstained for Nissl with *green fluorochrome*. Image shows labeling for Cx36 (*arrowheads*) at appositions between pairs of MesV neurons. Modified from Curti et al. (2012)

along a dorsoventral axis, thus reducing the frequency of contacts between them. Nevertheless, most of these neurons were moderately laden with fine Cx36-positive puncta around their periphery. At more posterior levels, the MesV nucleus is much more compact, with constituent somata often appearing in clusters and in close apposition to each other. Labeling associated with MesV somata consisted of both fine Cx36-positive puncta around the somata surfaces and large aggregates of puncta at points of contact (Fig. 1c, arrowheads). Through focus of entire cells by confocal microscopy revealed that virtually all of the fine dispersed puncta were localized to the cell surface rather than intracellularly (Curti et al. 2012).

As shown by confocal analysis (Fig. 2a), immunolabeling at somatic appositions did not consist of a single large immunopositive plaque, but rather of numerous small puncta. Aggregates of puncta at somatic appositions were often visualized on edge but were occasionally captured *en face* (Fig. 2a, top), revealing various features of their organization. Taking advantage of the uncommon opportunity of identifying the junctional area between two neurons (most electrical coupling in mammalian neurons generally occurs at remote dendro–dendritic contacts; Connors and Long 2004), we calculated the average area of labeling for Cx36 at somato–somatic contacts. As determined from *en face* views of Cx36 immunofluorescence at contact sites between MesV somata (Fig. 2a), the average number of Cx36-puncta per apposition was 70.1 ± 9.9 SEM, the puncta diameter was 0.34 ± 0.09 μm SEM, and the average puncta area was 0.36 ± 0.028 $\mu m^2$ SEM ($n = 10$) (Fig. 2b–d). Complete confocal reconstruction of these contacts areas allowed us to determine that labeling most frequently appeared at appositions linking pairs or triplets of somata (Curti et al. 2012).

Somatic appositions between MesV neurons at postnatal day 9 and in adult did not display any immunolabeling for all other connexins examined, including connexins found in various peripheral cell types such as Cx30.3, 31.1, Cx31, Cx37, Cx39, Cx40, Cx46 or Cx50 (not shown). Nor did these appositions display labeling for connexins (Cx26, Cx29, Cx30, Cx32, Cx43 and Cx47) expressed in glial cells (Nagy et al. 2004), as shown by examples of double immunofluorescence labeling for some of these connexins in combination with labeling for Cx36 (Fig. 3). Immunolabeling for Cx32 was localized to myelinated fibers traversing a region immediately adjacent laterally to the

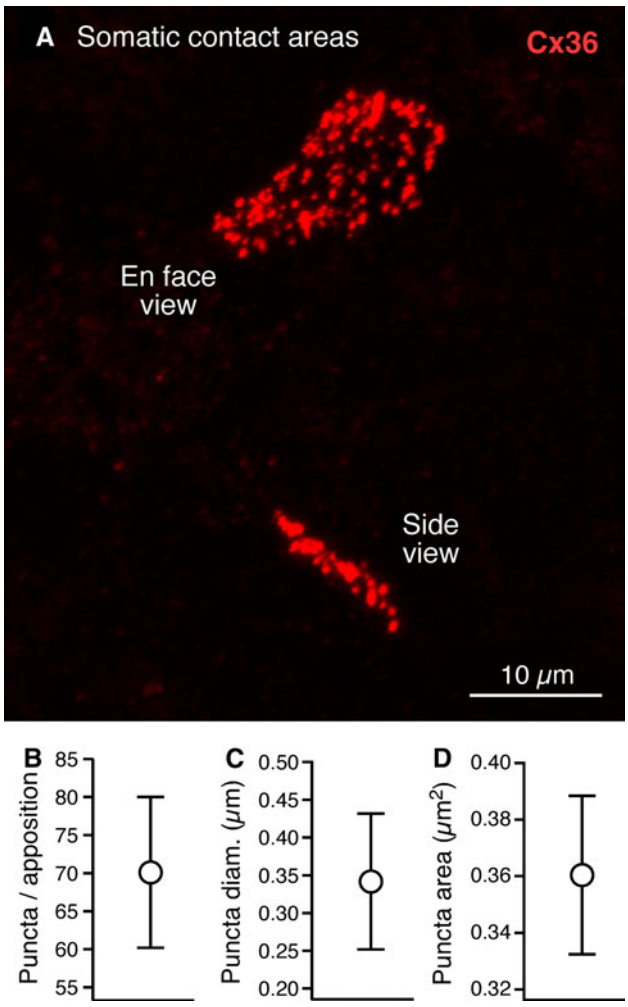


**Fig. 2** Quantification of Cx36 labeling at somatic contact areas. **a** Confocal immunofluorescence (z-stack) *en face* view and side view appositions between two different pairs of MesV neurons. Only *en face* views of Cx36-immunopositive clusters were used for quantitation of Cx36-puncta area at appositions between pairs of MesV neurons. **b** Average of puncta per apposition. **c** Average of puncta diameter. **d** Average of puncta area

MesV nucleus, and was absent in the MesV nucleus (Fig. 3a). Punctate labeling for Cx47 was localized to oligodendrocyte cell bodies intermingled with fibers lateral to the MesV nucleus (Fig. 3b). Labeling for Cx30 and Cx43, which occur at astrocyte gap junctions throughout the brain (Nagy et al. 2004), was found around the MesV nucleus and sparsely dispersed within the nucleus (Fig. 3c, d). None of these connexins were found to be colocalized with Cx36 at appositions between MesV neurons, as shown by image overlay of labeling for Cx36 in combination with each of these connexins (Fig. 3a–d). Examination of other connexins reported to be expressed in neurons of adult brain (i.e., Cx30.2, Cx45 and Cx57) also revealed an absence of these at MesV neuronal appositions, as shown in the case of labeling for Cx45, which was instead

**Fig. 3** Double immunofluorescence labeling of various connexins in combination with Cx36 in MesV nucleus at postnatal day 15 in rat brain. **a**, **b** Immunolabeling of the oligodendrocyte connexins Cx32 and Cx47 is restricted to myelinated fibers running lateral to the MesV nucleus (**A1**, *arrows*) and to oligodendrocyte cell bodies (**B1**, *arrowheads*), respectively; neither connexin is associated with MesV neurons or with Cx36 (**A2**, **B2**, *arrows*; and **A3**, **B3**, *overlay*). **c**, **d** Sparse immunolabeling of the astrocyte connexins Cx30 (**c**, *arrows*) and Cx43 (**d**, *arrows*) occurs within the MesV nucleus, where Cx36 is concentrated (**c**, **d**, *arrows*), and neither connexin is seen at MesV neuronal appositions or in association with Cx36 (**c**, **d**, *overlay*). **e** Punctate immunolabeling of Cx45 is restricted to blood vessels, in this case to a vessel traversing through the MesV nucleus (**E1**, *arrows*), and no labeling is seen associated with MesV neurons or with Cx36 (**E2**, *arrows*, and **E3** *overlay*). Scale bars = **a**, **b**, 100 μm; **c**, 10 μm; **d** 20 μm; **e**, 50 μm

localized along blood vessels traveling through the MesV nucleus (Fig. 3e), consistent with the expression of Cx45 by smooth muscle cells along vasculature elsewhere in brain (Kruger et al. 2000; Li and Simard 2001).

## Estimates of Junctional Conductance under Voltage Clamp

The large spherical cell bodies and the somatic location of the gap junctional area between these cells facilitates recording from these cells and provides unusual advantages for biophysical examination of the properties of native neuronal gap junctions. More specifically, and in contrast with other neuronal types, the somatic location of gap junctions and spherical geometry of MesV neurons as well as the fact they tend to be coupled in pairs, contribute to alleviate space clamp limitations. We therefore obtained direct measurements of junctional conductance from pairs of coupled cells by using the dual whole cell patch clamp technique. Current responses to voltage steps in a presynaptic neuron where recorded in a coupled postsynaptic MesV neuron (Fig. 4a), and the junctional conductance was obtained from the slope of V–I relationships (Fig. 4b) (Curti et al. 2012). Junctional conductance averaged 2.8 ± 2.0 nS SD, $n = 8$ (Fig. 5a). In pairs where it was possible to estimate conductance in both directions the values were largely symmetrical, corroborating the lack of significant rectification at these contacts obtained under current clamp conditions.

## Electrical Coupling is Supported by a Small Fraction of Open Gap Junction Channels

From the various measurements of labeled puncta (Fig. 2), we calculated the total Cx36 labeled area (area of all puncta) per apposition, which averaged 25.5 ± 3.9 $\mu m^2$ SEM (Fig. 5b). Because Cx36 was the only connexin detected at these contacts (Curti et al. 2012) and assuming

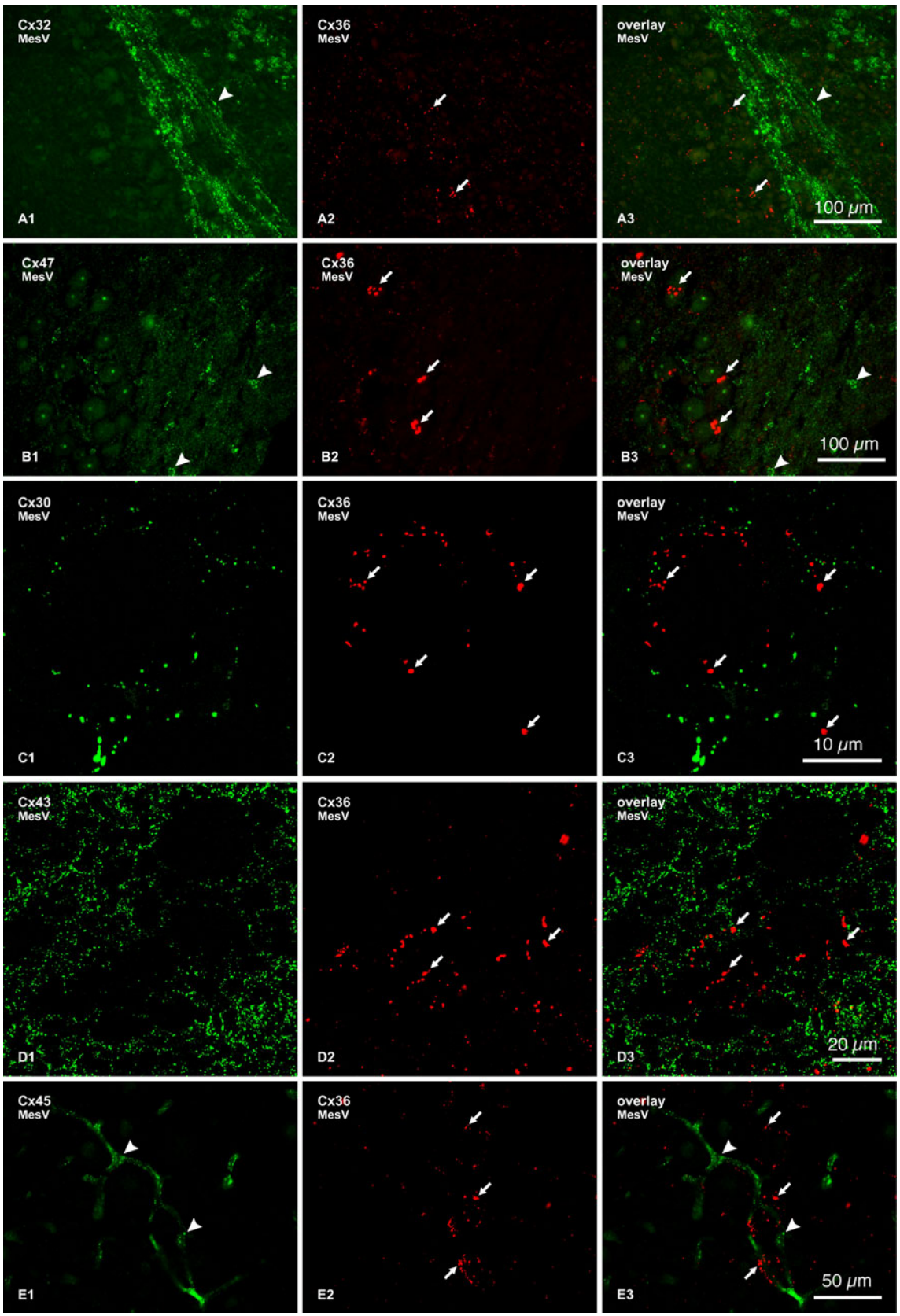
Cx32
MesV
A1
Cx36
MesV
A2
overlay
MesV
A3
100 μm
Cx47
MesV
B1
Cx36
MesV
B2
overlay
MesV
B3
100 μm
Cx30
MesV
C1
Cx36
MesV
C2
overlay
MesV
C3
10 μm
Cx43
MesV
D1
Cx36
MesV
D2
overlay
MesV
D3
20 μm
Cx45
MesV
E1
Cx36
MesV
E2
overlay
MesV
E3
50 μm

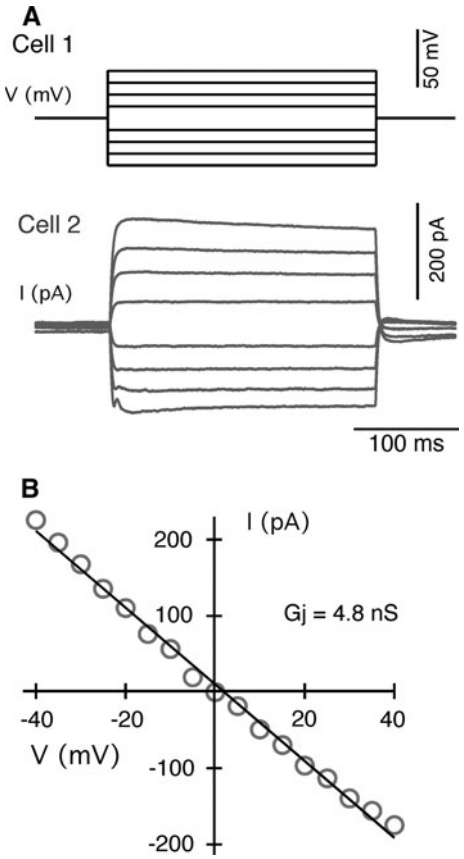


**Fig. 4** Determination of junctional conductance between coupled pairs of MesV neurons. **a** Current traces obtained under dual whole cell voltage clamp configuration. Both cells were held at −50 mV and voltage commands of increasing magnitude in steps of 5 mV of both polarities were applied to one of the cells (cell 1, *top*), while monitoring junctional current in the second cell (cell 2, *bottom*). The transient component observed in response to strong positive voltage commands corresponds to an undetermined voltage-dependent conductance of the presynaptic cell that is not blocked by TTX or $K^+$ channel blockers). **b** Graph of junctional current (ordinates) versus transjunctional voltage (abscissa) for the recordings depicted in (**a**). The data were fitted to a straight-line function and the junctional conductance (Gj) was determined from the slope of this linear regression (4.8 nS in this pair). Modified from Curti et al. (2012)

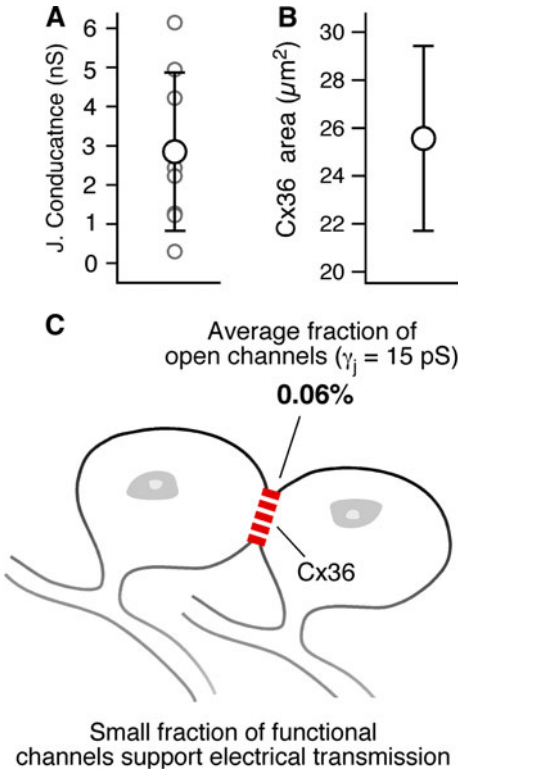


**Fig. 5** A small fraction of gap junction channels supports electrical transmission between pairs of MesV neurons. **a** Estimates of junctional conductance obtained under voltage clamp configuration. Individual (*open circles*) and average (*solid circles*) values are illustrated superimposed (*error bars* indicate SD). According to these estimates of macroscopic junctional conductance and assuming a unitary conductance ($\gamma_j$) of 10–15 pS, the average number of open channels is 190–280, representing the 0.06–0.09 % of the average total population. **b** Average of Cx36 labeling area per apposition at somatic contacts. Assuming a density of 12,000 connexons per square micrometer, the averaged labeled area represents 306,000 intercellular channels per contact between MesV neurons. **c** The cartoon illustrates that electrical transmission is supported by a small proportion of open gap junction channels at appositions between MesV neurons. Modified from Curti et al. (2012)

that connexons in gap junction plaques between MesV neurons are organized in a crystalline fashion, where the density is reported to be 12,000 connexons per $\mu m^2$ (Kamasawa et al. 2006), the labeled area corresponds to about 306,000 channels. Because the single channel conductance of gap junction channels formed by Cx36 was reported to be 10–15 pS (Srinivas et al. 1999b; Teubner et al. 2000), the values of junctional conductance indicate that the average number of open gap junction channels was of 190–280. Given that the opening probability of functional gap junction intercellular channels was reported to be close to 1 (Srinivas et al. 1999a), this estimate indicates that, on average, only 0.06–0.09 % of gap junction channels between MesV neurons are conductive. Independent estimates of junctional conductance between the same pairs of MesV neurons using indirect approaches which involve measurements of coupling coefficient and input resistance provided independent support for the notion that a very low fraction of open channels contribute to electrical coupling. Indirectly estimated junctional conductance averaged 7.3 ± 5.0 nS SD ($n = 9$), representing 0.16–0.24 % of the total population of channels, a value which was also consistent with estimates obtained with current clamp for all the coupled pairs. Finally, the differences in junctional conductance observed between pairs of MesV neurons would indicate that the number of open channels between cells could be varied.

## Discussion

Taking advantage of current electrophysiological approaches, our recordings from pairs of MesV neurons provided direct evidence for the existence of electrical coupling between neurons of the MesV nucleus (Curti et al. 2012). Electrical coupling was symmetrical and junctions non-rectifying. Strikingly, although unusually strong (Curti et al. 2012), coupling was supported by a small number of channels ($\sim$200), which represented a very small proportion ($\sim$0.1 %) of the gap junction channels estimated to be present at the contacts (Fig. 5c). These calculations were possible because of the advantageous experimental access of these electrical synapses: (1) unlike most electrical synapses in mammalian brain, which are located at remote dendritic processes, the ability to identify the areas of contact between MesV neurons made it possible to estimate the average number of channels between these neurons, (2) the organization of coupling in the nucleus mostly in pairs of coupled cells facilitated electrophysiological analysis, and (3) the spherical somata and proximity of electrodes to somatic gap junctions permitted more rigorous biophysical analysis, allowing us to estimate the average number of conductive channels responsible for electrical coupling (assuming a unitary conductance of 15 pS; Srinivas et al. 1999a). Because functional gap junction channels characteristically have an open probability of $\sim$1 at a transjunctional voltage of zero (Srinivas et al. 1999b), these results indicate that electrical transmission at these somatic contacts likely results from a small number of channels with a high open probability rather than from larger number of them with low open probability.

The estimated fraction of open channels was similar for independent estimates of junctional conductance, using either indirect (from measurements of coupling coefficient and input resistance) or direct (voltage clamp) approaches, supporting the notion that a small fraction of channels are conductive. On the other hand, it is important to emphasize that these estimates assume a unitary conductance of Cx36 channels, which has been similarly reported by various groups (Srinivas et al. 1999b; Teubner et al. 2000), but which has not been so far validated in a native neuronal gap junction. The small proportion of open channels found is consistent with similar estimates obtained at mixed synapses formed by afferent terminals on the goldfish Mauthner cell, where only a small percentage of channels ($\sim$1 %) support the electrical component of a unitary mixed synaptic potential (Lin and Faber 1988) and where the number of channels was obtained from direct ultrastructural reconstruction of these terminals (Tuttle et al. 1986). Further, a similar fraction of open Cx36 gap junction channels ($\sim$0.1 %) was obtained in expression systems combining electrophysiological and imaging approaches (F. Bukauskas, personal communication). Despite our use of indirect methods, this agreement between the present results and those derived from other approaches in Mauthner cells and transfected cells suggests that our estimates of channel number were not significantly affected by our assumptions.

Docking of connexons requires a specific distance between the membranes of adjoining cells, and cell–cell channels that did not open might therefore contribute to the mechanical stability necessary to maintain functional intercellular channels. In this view both, conductive and nonconductive channels would play important functional roles in electrical transmission. It has been recently shown that the strength of electrical transmission is maintained by a balance between hemichannel insertion, cell–cell channel formation, and channel removal with an overall half-life of $\sim$1–3 h (Flores et al. 2012), a value that is consistent with previous estimates for turnover of gap junctions in expression systems and intact tissue (Beardslee et al. 1998; Herve et al. 2007). The generation of such striking disparity between conductive and nonconductive channels may reflect essential aspects of gap junction formation and maintenance, which include the lifetime of intercellular gap junction channels and the existence of heterogeneous populations of these channels within the plaque.

On the other hand, it is clear that stable interneuronal gap junctions can form with a very small number of connexins present in the junction. At neuronal gap junctions in the retina, for example, linear arrays of scores of connexons in what have been termed string gap junctions consist of only one or two particles in width. These strings constitute true gap junctions because their constituent connexons are seen to be docked across apposing membranes (Kamasawa et al. 2006), although it is not known what proportion, if any, of the channels in string junctions reside in a open conducting state.

**Acknowledgments** Supported in part by Comisión Sectorial de Investigación Científica (to S.C.), National Institutes of Health (NIH) Grants DC03186 and NS0552827 (to A.E.P.), and NIH Grant NS44395 and Canadian Institutes of Health Research (to J.I.N). Also supported by the program "Vinculación con científicos y tecnólogos uruguayos residentes en el exterior" of Agencia Nacional de Investigación e Innovación, Uruguay.

## Reference

Baker R, Llinás R (1971) Electrotonic coupling between neurones in the rat mesencephalic nucleus. J Physiol 212:45–63

Beardslee MA, Laing JG, Beyer EC, Saffitz JE (1998) Rapid turnover of connexin43 in the adult rat heart. Circ Res 83:629–635

Bennett MVL (1997) Gap junctions as electrical synapses. J Neurocytol 26:349–366

Bennett MV, Pereda A (2006) Pyramid power: principal cells of the hippocampus unite! Brain Cell Biol 35:5–11

Bennett MV, Zukin RS (2004) Electrical coupling and neuronal synchronization in the mammalian brain. Neuron 41:495–511

Condorelli DF, Parenti R, Spinella F, Trovato Salinaro A, Belluardo N, Cardile V, Cicirata F (1998) Cloning of a new gap junction gene (Cx36) highly expressed in mammalian brain neurons. Eur J Neurosci 10:1202–1208

Connors BW, Long MA (2004) Electrical synapses in the mammalian brain. Annu Rev Neurosci 27:393–418

Curti S, Hoge G, Nagy JI, Pereda A (2012) Synergy between electrical coupling and membrane properties promotes strong synchronization of neurons of the mesencephalic trigeminal nucleus. J Neurosci 32:4341–4359

Flores C, Nannapaneni S, Davidson K, Yasumura T, Bennett MV, Rash JR, Pereda A (2012) Trafficking of gap junction channels at a vertebrate electrical synapse in vivo. Proc Nat Acad Sci USA 109:E573–E582

Herve JC, Derangeon M, Bahbouhi B, Mesnil M, Sarrouilhe D (2007) The connexin turnover, an important modulating factor of the level of cell-to-cell junctional communication: comparison with other integral membrane proteins. J Membr Biol 217:21–33

Hinrichsen CF (1970) Coupling between cells of the trigeminal mesencephalic nucleus. J Dent Res 49(6 suppl):1369–1373

Hinrichsen CF, Larramendi LM (1970) The trigeminal mesencephalic nucleus II. Electron microscopy. Am J Anat 127:303–319

Hormuzdi SG, Filippov MA, Mitropoulou G, Monyer H, Bruzzone R (2004) Electrical synapses: a dynamic signaling system that shapes the activity of neuronal networks. Biochim Biophys Acta 1662:113–137

Kamasawa N, Furman CS, Davidson KG, Sampson JA, Magnie AR, Gebhardt BR, Kamasawa M, Yasumura T, Zumbrunnen JR, Pickard GE, Nagy JI, Rash JE (2006) Abundance and ultrastructural diversity of neuronal gap junctions in the OFF and ON sublaminae of the inner plexiform layer of rat and mouse retina. Neuroscience 142:1093–1117

Kruger O, Plum A, Kim J-S, Winterhager E, Maxeiner S, Hallas G, Kirchhoff S, Traub O, Lamers WH, Willecke K (2000) Defective vascular development in connexin45-deficient mice. Development 127:4179–4193

Li X, Simard JM (2001) Connexin45 gap junction channels in rat cerebral vascular smooth muscle cells. Am J Physiol 281: H1890–H1898

Li X, Olson C, Lu S, Kamasawa N, Yasumura T, Rash JE, Nagy JI (2004a) Neuronal connexin36 association with zonula occludens-1 protein (ZO-1) in mouse brain and interaction with the first PDZ domain of ZO-1. Eur J Neurosci 19:2132–2146

Li X, Ionescu AV, Lynn BD, Lu S, Kamasawa N, Morita M, Davidson KG, Yasumura T, Rash JE, Nagy JI (2004b) Connexin47, connexin29 and connexin32 co-expression in oligodendrocytes and Cx47 association with zonula occludens-1 (ZO-1) in mouse brain. Neuroscience 126:611–630

Lin JW, Faber DS (1988) Synaptic transmission mediated by single club endings on the goldfish Mauthner cell. I. Characteristics of electrotonic and chemical postsynaptic potentials. J Neurosci 8:1302–1312

Llinas R (1975) Electrical synaptic transmission in the mammalian central nervous system. In: Santini M (ed) Proceedings of the golgi centennial symposium. Raven Press, New York, pp 379–386

Meier C, Dermietzel R (2006) Electrical synapses–gap junctions in the brain. Results Probl Cell Differ 43:99–128

Nagy JI, Dudek FE, Rash JE (2004) Update on connexins and gap junctions in neurons and glia in the mammalian nervous system. Brain Res Rev 47:191–215

Pedroarena CM, Pose IE, Yamuy J, Chase MH, Morales FR (1999) Oscillatory membrane potential activity in the soma of a primary afferent neuron. J Neurophysiol 82:1465–1476

Peinado A, Yuste R, Katz LC (1993) Gap junctional communication and the development of local circuits in neocortex. Cereb Cortex 3:488–498

Penes M, Li X, Nagy JI (2005) Expression of zonula occludens-1 (ZO-1) and the transcription factor ZO-1-associated nucleic acid-binding protein (ZONAB/MsY3) in glial cells and co-localization at oligodendrocyte and astrocyte gap junctions in mouse brain. Eur J Neurosci 22:404–418

Pereda AE, Rash JE, Nagy JI, Bennett MV (2004) Dynamics of electrical transmission at club endings on the Mauthner cells. Brain Res Rev 47:227–244

Söhl G, Degen J, Teubner B, Willecke K (1998) The murine gap junction gene connexin36 is highly expressed in mouse retina and regulated during brain development. FEBS Lett 428:27–31

Srinivas M, Costa M, Gao Y, Fort A, Fishman GI, Spray DC (1999a) Voltage dependence of macroscopic and unitary currents of gap junction channels formed by mouse connexin50 expressed in rat neuroblastoma cells. J Physiol 517:673–689

Srinivas M, Rozental R, Kojima T, Dermietzel R, Mehler M, Condorelli DF, Kessler JA, Spray DC (1999b) Functional properties of channels formed by the neuronal gap junction protein connexin36. J Neurosci 19:9848–9855

Teubner B, Degen J, Söhl G, Güldenagel M, Bukauskas FF, Trexler EB, Verselis VK, De Zeeuw CI, Lee CG, Kozak CA, Petrasch-Parwez E, Dermietzel R, Willecke K (2000) Functional expression of the murine connexin 36 gene coding for a neuron-specific gap junctional protein. J Membr Biol 176:246–249

Tuttle R, Masuko S, Nakajima Y (1986) Freeze-fracture study of the large myelinated club ending synapse on the goldfish Mauthner cell: special reference to the quantitative analysis of gap junctions. J Comp Neurol 246:202–211